

Modeling water diffusion in polybenzimidazole membranes using partial immobilization and free volume theory

Joshua D. Moon^a, Michele Galizia^b, Hailun Borjigin^c, Ran Liu^c, Judy S. Riffle^c, Benny D. Freeman^{d,*}, Donald R. Paul^d

^a California NanoSystems Institute, University of California, Santa Barbara, Elings Hall, Mesa Road, Santa Barbara, CA, 93106, USA

^b School of Chemical, Biological and Materials Engineering, The University of Oklahoma, 100 E. Boyd Street, Norman, OK, 73019, USA

^c Department of Chemistry, Macromolecules Innovations Institute, Virginia Tech, Blacksburg, VA, 24061, USA

^d John J. McKetta Jr. Department of Chemical Engineering, The University of Texas at Austin, 2501 Speedway, Austin, TX, 78712, USA

ARTICLE INFO

Keywords:

Diffusion
Plasticization
Free volume
Partial immobilization
Polybenzimidazole

ABSTRACT

This study extends previous work on modeling water sorption, dilation, and diffusion in polybenzimidazoles (PBIs) by comparing water transport properties of commercial PBI (Celazole®) with three sulfone-containing PBIs. A model is developed combining free volume and partial immobilization theories to describe water diffusion coefficients across a wide range of concentrations and degrees of swelling. Water vapor sorption and dilation follow dual-mode behavior and generally correlate with the availability of strong hydrogen bonding sites on the polymer chains. At low concentrations, water diffusion coefficients are suppressed by partial immobilization of Langmuir species, while at high concentrations, water diffusion coefficients increase due to significant swelling and plasticization. To account for the influence of plasticization on free volume and water mobility, local Henry's law mobility coefficients are correlated with fractional free volume (FFV), where the volume occupied by water molecules is considered to contribute to dynamic free volume and is assumed to be as accessible for water diffusion as unoccupied free volume. Contributions to diffusion coefficients from thermodynamic and convective frame of reference effects and concentration averaging are also considered.

1. Introduction

Numerous studies have correlated small molecule diffusion coefficients in polymers with polymer free volume, often following a model set forth by Cohen and Turnbull in 1959 and further extended by Vrentas and Duda in 1977 [1,2]. In this model, polymer chains have non-uniformly distributed void spaces (i.e., free volume elements) which can be occupied by small molecules, such as water [1–3]. As chains undergo cooperative segmental motion, small molecules execute diffusion jumps between free volume elements via an activated process and will diffuse through the polymer driven by a concentration (i.e., chemical potential) gradient [4,5]. In this model, molecular diffusion coefficients scale exponentially with reciprocal fractional free volume (FFV) [1–3,6].

More recent studies consider free volume to include both static and dynamic contributions [5,7–12]. Static contributions to free volume arise from chain stiffness and defects in molecular packing, which are enhanced in glassy polymers due to their non-equilibrium state [2,

13–17]. Dynamic contributions to free volume arise from local side group and coordinated chain motions and can be considered a time-dependent portion of free volume [5,7–11,18]. Thus, both the size distribution and concentration of pre-existing cavities from inefficient chain packing and local polymer chain dynamics impact free volume and diffusion of small molecules in polymers.

While many studies in the gas separation membrane literature have primarily studied the role of FFV in gas transport for neat, unplasticized polymers, often correlating gas transport properties of different molecular structures with differences in FFV, fewer studies have investigated the role of free volume in molecular transport for highly swollen or plasticized polymers. The non-equilibrium nature of glassy polymers makes their free volume properties particularly difficult to characterize, especially in the presence of a swelling penetrant.

Positron annihilation lifetime spectroscopy (PALS) has been occasionally employed to correlate small molecule diffusivity with FFV. Some studies suggest the addition of a highly sorbing penetrant to a polymer increases free volume by swelling the polymer and creating

* Corresponding author.

E-mail address: freeman@che.utexas.edu (B.D. Freeman).

<https://doi.org/10.1016/j.polymer.2020.122170>

Received 5 November 2019; Received in revised form 5 January 2020; Accepted 11 January 2020

Available online 13 January 2020

0032-3861/© 2020 Elsevier Ltd. All rights reserved.

new free volume sites, which has been observed for some polymer/plasticizer mixtures via PALS [13,18–22]. In contrast, other studies have suggested highly sorbing species occupy pre-existing free volume sites present in glassy polymers due to their non-equilibrium state and instead reduce FFV, which has also been observed for polymer/penetrant mixtures via PALS [12,13,23–25]. Often, this FFV reduction, associated with antiplasticization, occurs at low penetrant concentrations, while an increase in FFV associated with plasticization occurs at high penetrant concentrations [13,23,24,26]. For example, in relatively non-polar polymers, such as Matrimid® (a polyimide), water uptake reduces free volume at all humidities, since effects of plasticization are negligible [18,24,26].

Without using techniques like PALS, estimating the amount of free volume in a swollen polymer is non-trivial, since it requires accurate knowledge of the extent of swelling of the polymer and the volume occupied by the swelling penetrant inside the polymer matrix [27]. Furthermore, correlating swollen polymer free volume with molecular diffusion coefficients is complicated by the fact that species sorbing into glassy polymers via Langmuir sorption often exhibit lower diffusion coefficients than those that sorb via Henry's law, a behavior known as partial immobilization [28–31]. While partial immobilization theory is often applied to penetrants at low concentrations, few studies discuss partial immobilization at high penetrant concentrations.

This study attempts to characterize the impact of water concentration on the free volume and diffusion properties of a series of glassy polybenzimidazoles (PBIs). Further, this study analyzes free volume using macroscopic water vapor sorption and dilation measurements, rather than relying on PALS measurements. Previously, we used these techniques to correlate water diffusion coefficients with FFV in PBIs by considering both unoccupied free volume and volume occupied by sorbed water molecules to be accessible for diffusion [32]. PBIs were chosen due to their interest for high performance gas separation membranes [33–40] and uniquely hydrophilic properties, exhibiting up to 25% liquid water uptake at 35 °C [32,38,41–43]. From a practical point of view, many industrial gas separation processes of interest for PBI membranes, such as syngas separation, operate with humidified gas streams, so it is important to understand the influence of water uptake on PBI transport properties, which has not been the focus of much study.

Previously, we reported water vapor sorption and dilation followed dual-mode behavior in commercial PBI (Celazole®) and a sulfone-containing PBI (TADPS-TPA) [32]. Water vapor diffusion coefficients increased with concentration in both PBIs, indicating plasticization caused by extensive water uptake [32]. In this study, we examine in greater detail the relationship between water uptake, plasticization, free volume, and diffusion in PBIs. Water vapor sorption, diffusion, and swelling were measured for two additional sulfone-containing PBIs, TADPS-IPA and TADPS-OBA, from near infinite dilution (i.e., 0.005 vapor activity) to high activities (i.e., 0.65 vapor activity). We hypothesize that water molecules fill some existing free volume while also swelling the polymer and contributing to the formation of additional free volume, which is speculated to arise from increased chain mobility. Furthermore, we attempt to combine partial immobilization and free volume theories to describe concentration-averaged water diffusion coefficients across a wide range of concentrations in PBIs.

Since PBIs have high affinity for water and undergo strong hydrogen bonding with sorbed water [43], diffusion coefficients are corrected for thermodynamic effects to isolate the effects of water mobility and chemical interactions on diffusion. Convective frame of reference effects at high water uptake levels are also considered. The contribution of each of these phenomena to observed water vapor diffusion coefficients is modeled and presented as a function of concentration for each PBI.

2. Experimental methods

2.1. Materials

The structures of the PBIs used in this study are presented in Fig. 1. TADPS-TPA, TADPS-IPA, and TADPS-OBA were synthesized as described previously [38]. Celazole S26 dope was purchased from PBI Performance Products Inc. and contains 26 wt% PBI solids in *N,N*-dimethylacetamide (DMAc) with 1.5 wt% LiCl added to improve PBI solubility. DMAc and *n*-heptane were purchased from Sigma-Aldrich and used without further purification. Deionized water was produced using a Millipore RiOS and A10 water purification system.

2.2. Membrane preparation

Dense films of TADPS-TPA, TADPS-IPA, and TADPS-OBA were formed using solution casting as described previously [38]. Celazole® films were cast similarly by diluting the S26 dope to 2.5 wt% PBI by adding DMAc and stirring until dissolved. The dilute Celazole® solution was filtered through a 0.45 µm PTFE filter and sonicated for 30 min to remove bubbles. The solution was poured into glass rings caulked onto a glass plate and placed on a level surface inside a vacuum oven. Solid films were formed by evaporating the solvent overnight under full vacuum at room temperature followed by 4 h at 80 °C and 1 h at 100 °C. Films were removed from the glass plate and boiled in deionized water for 4 h to remove any residual DMAc from the films. Finally, films were dried at full vacuum at 150 °C for at least 24 h. Solvent removal was previously verified by TGA [32].

2.3. Water vapor gravimetric sorption

Water vapor sorption measurements for TADPS-IPA and TADPS-OBA were performed with a McBain quartz spring balance as described previously [32,44,45]. PBI films were cut into small pieces about 20 µm thick and a few square centimeters in area and suspended from a quartz spring (Ruska Instrument Corporation) inside a jacketed glass vacuum chamber. The jacket temperature was maintained at 35 °C using a water circulator. Film thicknesses were measured with digital calipers (Mitutoyo, ± 1 µm resolution). Each sample was degassed under full vacuum

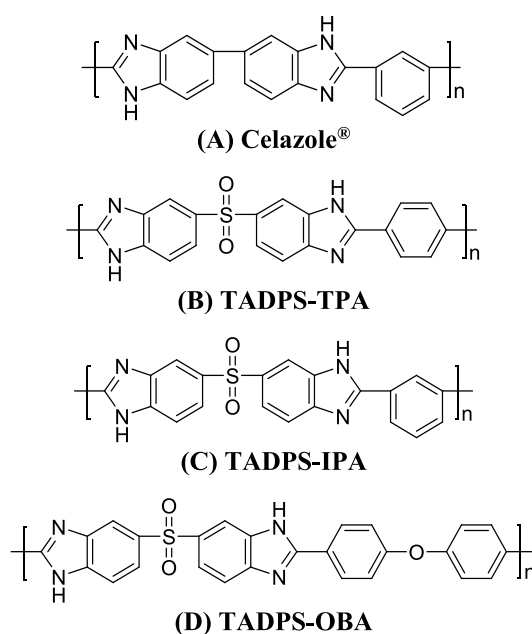


Fig. 1. Molecular structures of (A) Celazole®, (B) TADPS-TPA, (C) TADPS-IPA, and (D) TADPS-OBA.

for at least three days prior to exposing them to water vapor during the first step of a sorption experiment.

Water vapor was generated from a glass reservoir containing deionized water connected to the system. Before each test, the reservoir was degassed for a couple minutes under vacuum to remove dissolved gases and air. MKS Baratron 626B transducers (full scale = 10 or 100 Torr, accuracy = 0.25% of full scale) were used to monitor water vapor partial pressure. Spring length was constantly monitored using a CCTV camera and IC Capture software (The Imaging Source) [46]. Images were processed via ImageJ software.

Integral sorption tests for TADPS-IPA and TADPS-OBA were run, where each sorption step was followed by a desorption step to full vacuum (i.e., zero vapor activity). Multiple sorption steps were run between 0.005 and 0.65 vapor activity for each polymer, where vapor activity is defined as the ratio of water vapor partial pressure to its saturation vapor pressure. Each step lasted approximately 2–3 days or until water uptake appeared to reach equilibrium. At very low activities, a slow pressure increase was observed during equilibration which was attributed to a slow air leak into the system. To mitigate uncertainty in vapor activities due to changing water partial pressure, equilibrium mass uptake was recorded after only a few hours for low activity measurements before the pressure was observed to increase. Negligible additional water uptake was observed at these low activities over the next few days of sample equilibration.

2.4. Water vapor dilatometry

Dilation of TADPS-IPA and TADPS-OBA was measured using an optical method as described previously [32]. Each PBI film was cut into a long thin strip approximately ~8 cm long x 0.3 cm wide with a thickness of around 20 μm . The strip was placed in the jacketed glass vacuum chamber used for gravimetric sorption measurements. The jacket temperature was maintained at 35 °C using a water circulator. A guide rod gently held each strip using thin copper wires to prevent the strip from curling during swelling while permitting it to elongate freely. Samples were degassed under full vacuum for at least a day prior to exposing them to the first activity of water vapor.

Integral dilation tests for TADPS-IPA and TADPS-OBA were run. For each dilation step, the sample was equilibrated with water vapor at a specified activity, then degassed under full vacuum (i.e., zero activity) for at least 24 h. Multiple dilation steps were run between 0.005 and 0.65 activity for each polymer. The length of the PBI strip was constantly monitored using a CCTV camera and IC Capture software (The Imaging Source) [46]. Images were processed via ImageJ software. The length of each sample was measured at different activities and converted to volumetric dilation by assuming isotropic swelling [32,47–49]:

$$\frac{\Delta V}{V_0} = \left(\frac{L_{\text{eqib}}}{L_{\text{dry}}} \right)^3 - 1 \quad (1)$$

where L_{eqib} is sample length after swelling, and L_{dry} is sample length before swelling (i.e., at zero water vapor activity). $\Delta V/V_0$ is the fractional volume change of the sample (i.e., volumetric dilation). Isotropic swelling was assumed since these polymers are generally considered to be amorphous and unoriented [32,38].

2.5. Density

TADPS-IPA and TADPS-OBA samples were loaded into stainless steel Swagelok chambers equipped with isolation valves. The chambers were placed in a vacuum oven with isolation valves open and dried under full vacuum at 35 °C for several days. The oven was purged with dry air passed through a Drierite column. The oven was then briefly opened, and isolation valves were immediately sealed to inhibit moisture from entering the chambers. The sealed chambers were placed into a glovebox purged with dry nitrogen. Humidity was maintained below 0.1%

inside the glovebox as measured by a digital hygrometer (Fisher Scientific, $\pm 2\%$ RH accuracy). Samples were removed from the stainless steel chambers, and their densities were measured inside the glovebox using a balance equipped with a density kit (Mettler Toledo) [50]. *n*-Heptane was used as the buoyant liquid, which has negligible uptake in PBIs [32].

3. Results and discussion

3.1. Water vapor sorption

Water vapor sorption isotherms for Celazole®, TADPS-TPA, TADPS-IPA, and TADPS-OBA at 35 °C are shown in Fig. 2. Sorption results for Celazole® and TADPS-TPA are from a previous study [32]. All sorption isotherms follow typical dual-mode behavior at water vapor activities up to 0.6, with TADPS-TPA and TADPS-OBA showing slightly upward curvature at the highest activities measured [32]. Vapor sorption at activities greater than ~0.65 could not be measured due to condensation of water vapor in slightly colder regions of the spring balance, which resulted in pressure fluctuations.

The dual-mode model for small molecule concentration in glassy polymers is given by [14]:

$$C = k_D p + \frac{C_H b p}{1 + b p} \quad (2)$$

where C is the equilibrium concentration in the film defined with respect to the volume of the dry film ($\text{cm}^3(\text{STP})/\text{cm}^3$ dry film), k_D is the Henry's law constant ($\text{cm}^3(\text{STP})/\text{cm}^3\text{atm}$), C_H is the Langmuir capacity ($\text{cm}^3(\text{STP})/\text{cm}^3$), b is the Langmuir affinity ($1/\text{atm}$), and p is the partial pressure of water vapor at equilibrium (atm). Dual-mode parameters were calculated using weighted regression in Mathematica and are recorded in Table 1 [32]. There is higher uncertainty for TADPS-TPA's dual-mode parameters, since only a small number of measurements were made below 0.2 activity where most Langmuir sorption occurs.

Langmuir capacities, C_H , increase in the following order: TADPS-OBA < TADPS-IPA < TADPS-TPA < Celazole®. C_H often correlates with the amount of non-equilibrium excess free volume in glassy polymers [14–17,51]. Non-equilibrium excess free volume decreases as temperature approaches the polymer's glass transition temperature and becomes zero at T_g [14,17]. Consequently, C_H is zero at or above T_g and typically increases as the difference between T and T_g increases. Thus, at a given temperature, one would generally expect C_H to be larger for polymers with a higher T_g [52,53]. The T_g s of the polymers in this study increase in the following order: Celazole® (417 °C), < TADPS-OBA (428 °C) < TADPS-IPA (447 °C) < TADPS-TPA (480 °C) [38]. Celazole®'s C_H is larger than expected based on its T_g , suggesting other phenomena may be affecting its Langmuir sorption.

Dry PBI fractional free volumes (FFV) were calculated from polymer dry densities and Bondi's group contribution parameters and increase in the following order: TADPS-IPA (0.107) < Celazole® (0.120) \approx TADPS-TPA (0.122) \approx TADPS-OBA (0.123) [32,54,55]. While C_H is often higher for polymers with higher FFV, there is no discernable trend between FFV and C_H in this case [14–17,51]. A small (i.e., 2–3 wt%) amount of residual water is present in PBIs even following extensive drying at 35 °C, and the presence of this strongly bound water may slightly affect measured densities and FFV values [32]. These strongly bound water molecules are irreversibly bound at 35 °C and are assumed not to contribute to sorption or dilation isotherms [32].

Water molecules interact with imidazole groups on the PBI backbone via strong hydrogen-bonding [32,41–43,56–58]. Introducing functional groups such as sulfone or ether groups into the PBI backbone reduces the molar density of imidazole groups, likely reducing the amount of strong hydrogen bonding occurring between water and the polymer. The molar density of imidazole nitrogen groups increases in the following order:

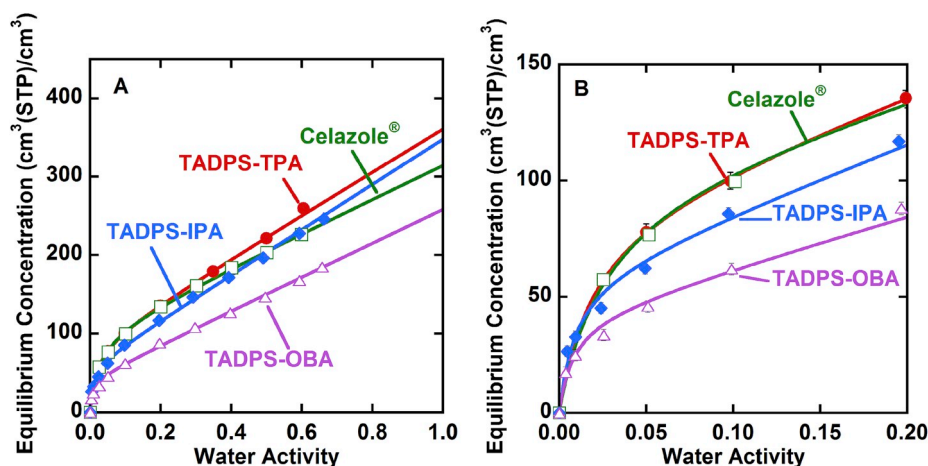


Fig. 2. Water vapor sorption isotherms for PBIs at 35 °C as a function of vapor activity. Lines represent dual-mode fits (Equation (2)). Right plot highlights activities between 0 and 0.2. Celazole® and TADPS-TPA data are from previous study [32].

Table 1

Water vapor dual-mode parameters and free volumes for PBIs at 35 °C.

	k_D [cm ³ (STP)/ cm ³ atm]	C'_H [cm ³ (STP)/ cm ³]	b [1/ atm]	PBI density [g/cm ³]	FFV
Celazole® [32]	3870 ± 140	102 ± 5	670 ± 90	1.270 ± 0.014	0.120 ± 0.010
TADPS-TPA [32]	4940 ± 380	88 ± 10	940 ± 470	1.362 ± 0.015	0.122 ± 0.010
TADPS-IPA	5110 ± 140	62 ± 3	1860 ± 300	1.385 ± 0.013	0.107 ± 0.008
TADPS-OBA	3740 ± 130	46 ± 3	1760 ± 370	1.341 ± 0.010	0.123 ± 0.007

TADPS-OBA (0.0116 mol N or N-H groups per cm³ polymer) < TADPS-TPA (0.0146 mol/cm³) ≈ TADPS-IPA (0.0149 mol/cm³) < Celazole® (0.0165 mol/cm³). Values of C'_H also increase in a similar order, suggesting Langmuir capacity may be somewhat influenced by the concentration of strong hydrogen bonding sites on the polymer backbone.

TADPS-OBA has the lowest water uptake and Henry's law constant of the four PBIs, likely due to its lower molar density of imidazole groups that results in less strong polymer-penetrant hydrogen bonding. TADPS-TPA and TADPS-IPA have similar Henry's law constants due to their isomeric similarity, and both exhibit higher Henry's law constants and lower Langmuir capacities than Celazole® [32]. The presence of sulfone groups may affect water uptake at low and high concentrations differently. At low concentrations, where Langmuir sorption dominates, most water molecules likely form hydrogen bonds with the imidazole groups [43]. Since the addition of sulfone groups reduces the density of strong hydrogen bonding sites on the polymer backbone, TADPS-based PBIs generally show lower water uptake at low activities compared to Celazole® and exhibit reduced Langmuir capacities.

At high concentrations, many strong hydrogen bonding sites are saturated with water (i.e., first-shell water), and additional water molecules are more likely to sorb into the polymer as second-shell water molecules, which primarily form hydrogen bonds with first-shell water molecules rather than with polymer chains [43]. Accommodating this additional sorbed water requires some polymer dilation [32]. The sulfone groups may increase water uptake in TADPS-IPA and TADPS-TPA relative to Celazole® by providing additional flexibility to the polymer backbone, allowing additional water molecules to fit between polymer

chains and increasing their Henry's law constants [32]. TADPS-based PBIs show enhanced solubility in polar solvents such as *N*-methyl-2-pyrrolidone and *N,N*-dimethylacetamide relative to Celazole®, so their sulfone groups may provide additional degrees of freedom to the polymer chains that increase small molecule solubility through an increase in configurational entropy [38].

3.2. Water-induced dilation

The degree of swelling, or volumetric dilation, of the four PBIs was measured using water vapor dilatometry. Dilation data for Celazole® and TADPS-TPA were reported previously [32]. Volumetric dilation isotherms of each PBI at activities ranging from 0.005 to about 0.65 are presented in Fig. 3. Above 0.1 activity, volumetric swelling increases linearly with activity for all PBIs. TADPS-IPA shows a slight deviation from linearity at the highest activity (~0.65). Consistent with previous observations for Celazole® and TADPS-TPA, TADPS-IPA and TADPS-OBA dilation isotherms show downwards curvature at activities below 0.1 [32]. This behavior suggests water molecules sorbing via the Langmuir mechanism contribute slightly to swelling in addition to the swelling afforded by molecules sorbing via the Henry's law mechanism [49,59]. Sorption and dilation follow the same order, with both increasing as follows: TADPS-OBA < Celazole® < TADPS-IPA < TADPS-TPA. As expected, extent of swelling correlates with water uptake.

Dilation isotherms were fit using a two parameter dual-mode dilation model by Punsalan and Koros:

$$\frac{\Delta V}{V_0} = V_D \left(k_D p + \frac{f C'_H b p}{1 + b p} \right) \quad (3)$$

where V_D is the effective condensed water molar volume (cm³/mol), and f is an empirical fitting parameter varying from 0 to 1 that represents the fraction of water molecules in Langmuir sites that require polymer matrix dilation (i.e., the average amount of dilation that results from a water molecule sorbing into a Langmuir site expressed as a fraction of V_D) [32,49,60]. Fitting parameters for Equation (3) were calculated using weighted regression of dilation data in Mathematica and are summarized in Table 2 [32]. The dual-mode sorption parameters used in Equation (3) (k_D , C'_H , and b) were taken from Table 1. V_D values were similar for all four PBIs and varied from 10.3 to 12.7 cm³/mol. Values of f were close to 0.3 for all polymers except TADPS-TPA, which showed a lower value of 0.17. The lower value of f for TADPS-TPA is possibly a mathematical artifact, since fewer data points for TADPS-TPA dilation were available for curve fitting in the low vapor activity range where Langmuir sorption dominates.

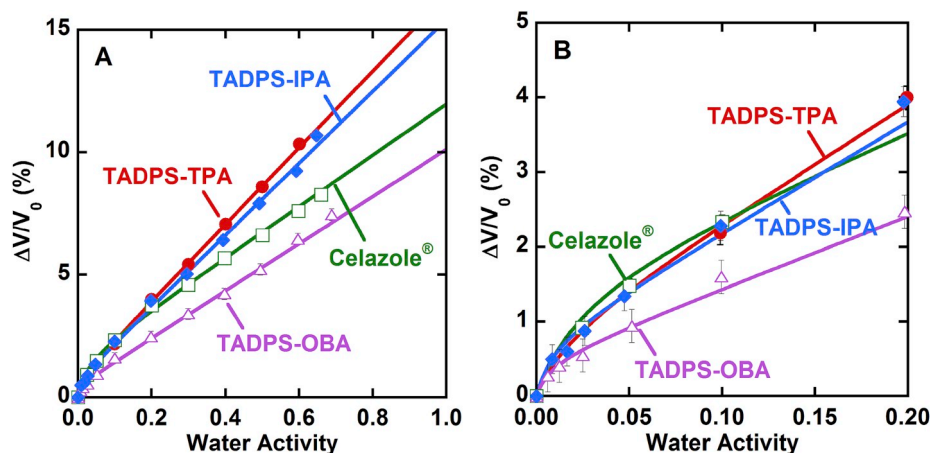


Fig. 3. Water vapor dilation for PBIs as a function of vapor activity at 35 °C. Lines represent dual-mode dilation model fits (Equation (3)). Right plot highlights activities between 0 and 0.2. Celazole® and TADPS-TPA data are from a previous study [32].

Table 2

Dual-mode dilation model parameters for PBI swelling.

	V_D [cm ³ /mol]	f
Celazole® [32]	10.8 ± 0.3	0.33 ± 0.03
TADPS-TPA [32]	12.7 ± 0.5	0.17 ± 0.05
TADPS-IPA	11.1 ± 0.3	0.32 ± 0.05
TADPS-OBA	10.3 ± 0.5	0.28 ± 0.08

3.3. Water partial molar volumes

Dual-mode parameters from sorption and dilation can be used to calculate water vapor partial molar volumes in PBIs as a function of pressure [32,47,60–63]:

$$\bar{V}_w \approx -\frac{\partial \left(\frac{\Delta V}{V_0} \right)}{\partial C} = V_D \frac{k_D + \frac{fC_D^b}{(1+bC)^2}}{k_D + \frac{C_D^b}{(1+bC)^2}} \quad (4)$$

Derivation of Equation (4) can be found in previous work [32]. Equation (4) was evaluated for each PBI at different concentrations using parameters from Tables 1 and 2. Fig. 4 shows water partial molar volumes as a function of equilibrium water concentration in the polymer. Water partial molar volumes for all four PBIs exhibited similar trends. At low concentrations, water molecules primarily sorb into

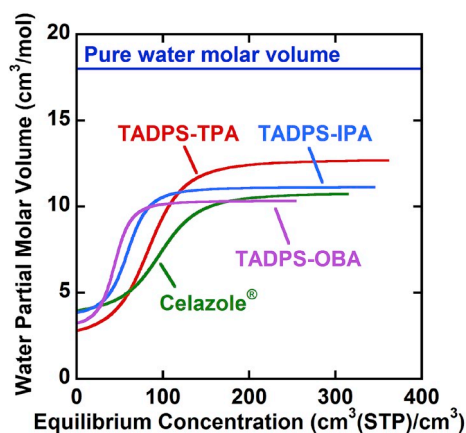


Fig. 4. Water vapor partial molar volumes in PBIs at 35 °C as a function of equilibrium concentration calculated using dual-mode sorption and dilation parameters (Equation (4)). Celazole® and TADPS-TPA data are from previous study [32].

Langmuir sites, which results in little swelling and low partial molar volumes. As these Langmuir sites become saturated at higher concentrations, more swelling occurs, and partial molar volume increases. At high concentrations, partial molar volumes approach the effective condensed molar volume of water (V_D), which varies slightly by PBI [32]. All PBIs exhibited effective condensed molar volumes of water significantly less than the molar volume of pure liquid water (18 cm³/mol) [32,63]. Small water molecules that undergo Henry's law sorption likely fit into interstitial spaces around rigid PBI segments, especially those which hydrogen-bond with imidazole groups, while other water molecules fill larger excess free volume elements (i.e., Langmuir sites) formed by inefficient packing of the highly aromatic PBI chains [20]. While some increase in volume is required to accommodate these water molecules (represented by V_D at high water concentrations), the volume change is less than that required in pure liquid water (i.e., 18 cm³/mol) where all molecules are small and there are fewer packing defects to be filled [32,63].

3.4. Water diffusion kinetics

Water diffusion coefficients in the four PBIs were calculated using kinetic uptake data from sorption measurements as described previously [32]. A modified version of the Berens-Hopfenberg model was applied which takes into account a slight delay in water uptake in the films due to non-instantaneous introduction of water vapor to the samples [16,32,64–67]. This model can also describe a slow water uptake process that occurs at longer time scales than Fickian diffusion and is ascribed to slow relaxation of the polymer segments. Water diffusion coefficients are shown as a function of vapor activity and average water concentration in the films in Fig. 5. Average concentration is defined as half of the equilibrium concentration at each activity. All diffusion coefficients increase with increasing water concentration in the films, indicating water has a strong plasticizing effect on all four PBIs.

TADPS-OBA exhibited the highest diffusion coefficients of the four PBIs at any given concentration. TADPS-OBA also has the highest gas permeabilities at 35 °C, which is ascribed to its greater chain flexibility and more disrupted chain packing afforded by its ether linkage [38,68]. TADPS-OBA has the highest free volume of the PBIs tested (0.123), which can contribute to higher diffusion coefficients [1,53,69,70].

Infinite dilution diffusion coefficients, D_∞ (estimated in a later section and shown in Table 3), increase in the following order: Celazole® < TADPS-TPA ≈ TADPS-IPA < TADPS-OBA. This trend agrees with the order of gas permeabilities previously reported for sulfone-containing PBIs [38]. TADPS-TPA has slightly higher gas permeabilities than TADPS-IPA, which is believed to be due in part to less efficient chain packing of the more linear *para*-linked phenyl group in TADPS-TPA,

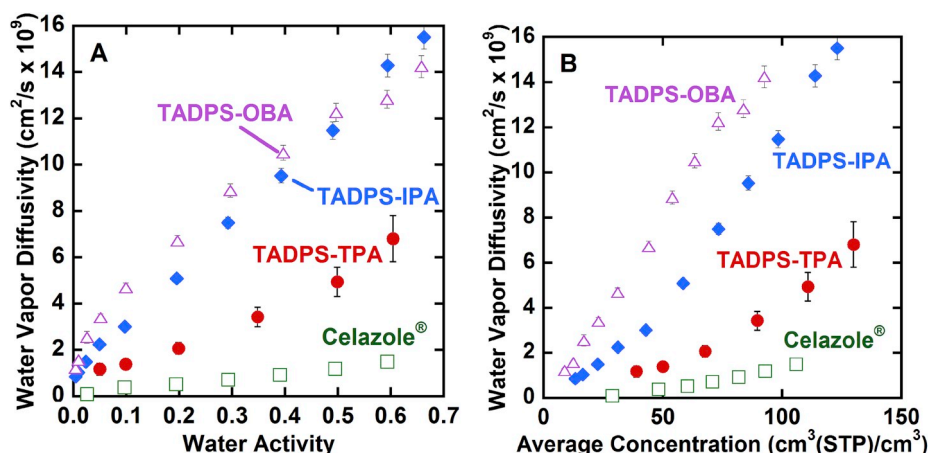


Fig. 5. Water vapor diffusion coefficients in PBIs at 35 °C as a function of: (A) vapor activity and (B) average water concentration in polymer. Diffusion coefficients were calculated using modified Berens-Hopfenberg model (fitting procedure described previously) [32]. Celazole® and TADPS-TPA data are from a previous study [32].

Table 3

Diffusion model parameters for Equation (12) and infinite dilution diffusion coefficients.

	$L_{loc,D,0}$ [cm ² /s x 10 ⁶]	B	$L_{loc,H}$ [cm ² /s x 10 ⁹]	$L_{loc,D,\infty}$ [cm ² /s x 10 ⁹]	D_{∞} [cm ² /s x 10 ⁹]
Celazole®	0.19	0.71	0.079	0.50	0.10
TADPS-TPA	2.29	0.97	0.61	0.80	0.63
TADPS-IPA	0.43	0.49	0.46	4.4	0.63
TADPS-OBA	0.19	0.38	0.68	8.9	1.04

resulting in its higher FFV than TADPS-IPA (i.e., 0.122 vs. 0.107) [38, 71–74]. The *para*-linked phenyl group in TADPS-TPA also has greater segmental mobility than the *meta*-linked phenyl group in TADPS-IPA, since it can undergo less sterically hindered rotation. This enhanced segmental mobility often leads to greater gas permeabilities for *para*-linked aromatic polymers vs. their *meta*-linked isomers [38,71,72,74]. However, in the present study, the infinite dilution water diffusion coefficients of TADPS-TPA and TADPS-IPA were very similar, and TADPS-IPA had greater diffusion coefficients than TADPS-TPA at higher concentrations by about a factor of two. Since water swells these PBIs at high activities, the presence of high concentrations of water could also significantly enhance PBI segmental mobility. Thus, segmental mobility can be affected both by water-induced plasticization and by sterics of functional groups in the polymer backbones.

TADPS-TPA and TADPS-IPA both swell by similar amounts at each activity (cf. Fig. 3). If TADPS-IPA is more strongly affected than TADPS-TPA by additional chain mobility from plasticizing water species, this effect may dominate over any hindered local segmental mobility due to steric hindrance of TADPS-IPA's *meta*-oriented phenyl group. The net result is higher diffusion coefficients for TADPS-IPA when plasticized by water.

Celazole® showed much lower water diffusion coefficients than its sulfone-containing analog (i.e., TADPS-IPA), despite having a higher FFV (0.120 vs. 0.107). This behavior likely results from Celazole®'s more restricted chain mobility due to the absence of sulfone groups. Additional degrees of motion afforded by sulfone groups that were potentially responsible for TADPS-IPA's increased Henry's law solubility due to an increase in configurational entropy may also be responsible for TADPS-IPA's increased diffusion coefficients. Sulfone-containing PBIs may be able to undergo a greater variety of chain motions than Celazole®, opening transient gaps between free volume elements more

frequently, thereby enabling faster water diffusion. Similar trends were observed for gas permeabilities in Celazole® and TADPS-IPA, where TADPS-IPA exhibited higher gas permeabilities at 35 °C than Celazole® [68].

3.5. Free volume theory

Molecular diffusion in polymers scales exponentially with fractional free volume (FFV) [1–3,6]:

$$D = A \exp\left(\frac{-B}{FFV}\right) \quad (5)$$

where A and B are empirical fitting parameters. In the absence of a swelling penetrant, FFV is generally defined as [69,75,76]:

$$FFV = \frac{V_{free}}{V} = 1 - \frac{V_{0,poly}}{V} \quad (6)$$

where V_{free} is the free volume in the polymer matrix available for penetrant diffusion, $V_{0,poly}$ is the occupied volume of the polymer segments, typically approximated via group contribution theory using the van der Waals volumes of monomer functional groups, and V is the total polymer volume [55,77,78].

In glassy polymers, changing polymer structure can affect both permeability and diffusion coefficients of gases and vapors due to changes in FFV (solubilities are generally less affected by free volume changes than diffusion and permeability coefficients) [53,69]. The free volume of a polymer with sorbed penetrant can be significantly different from that of a penetrant-free polymer, since the sorbed penetrant can change the number and size of free volume elements available in the polymer matrix for diffusion. Koros and Paul argued that the Langmuir portion of sorbed gas or vapor species occupies frozen unoccupied volume (i.e., excess non-equilibrium free volume) present as local inhomogeneities in the polymer matrix [12,14–17,20]. As a result, polymer/penetrant mixtures can have higher densities and lower FFV values than those of the pure polymer (i.e., antiplasticization) [24,78,79].

Additionally, sorbed molecules can disrupt polymer/polymer interactions and create new, weaker polymer/penetrant interactions, and high concentrations of sorbed penetrants can swell the polymer, increase chain mobility, and reduce the T_g of the polymer/penetrant mixture [12, 23–25]. This is in contrast to antiplasticization behavior at low penetrant concentrations. Several studies report plasticizer addition simultaneously reduced PALS free volumes and decreased mixture T_g [12, 23–25]. Molecular diffusion was faster in these plasticized polymers

compared to their unplasticized state, which cannot be explained by a purely static definition of free volume. It was concluded that the addition of plasticizer contributed to the formation of dynamic free volume that was accessible for transport due to the high frequency of penetrant motion [12,23].

There are two limiting cases useful for estimating the amount of FFV in a plasticized polymer that is accessible for diffusion. In one case, the volume occupied by penetrant molecules (e.g., water) is available for chain motion and molecular diffusion and, therefore, contributes to fractional free volume. The fractional free volume in this case (FFV) is defined as follows [32,80]:

$$FFV = 1 - \frac{V_{0,poly}}{V_{mixture}} \quad (7)$$

where $V_{0,poly}$ is the volume occupied by the polymer chains, and $V_{mixture}$ is the volume of the swollen polymer-penetrant mixture. In this limit, the penetrant does not contribute to occupied volume. This case attempts to account for additional dynamic contributions to free volume arising from plasticization-induced increases in molecular mobility.

In the other limiting case, the volume occupied by penetrant molecules contributes to the occupied volume of the polymer-penetrant mixture and does not increase the free volume accessible for diffusion. The fractional free volume where the penetrant contributes to the occupied volume of the polymer-penetrant mixture (FFV*) is defined as follows [2,26,27,78].

$$FFV^* = 1 - \frac{V_{0,poly}}{V_{mixture}} - \frac{V_{0,penetrant}}{V_{mixture}} \quad (8)$$

where $V_{0,penetrant}$ is the volume occupied by sorbed penetrant (e.g., water). This approach assumes additivity of specific occupied volumes of polymer and penetrant and is a primarily static definition of free volume based on molecular packing.

Both limiting cases can be evaluated for water-swollen PBIs, where the volume occupied by sorbed water (i.e., the penetrant in Equations (7) and (8)) is either excluded or included in the free volume calculation. Values of FFV and FFV* were calculated at different sorbed water concentrations using sorption and dilation dual-mode parameters as described previously [32]. FFV calculated from Equation (7) increases with concentration (cf., Fig. 6), while FFV* calculated from Equation (8) decreases with concentration. Previous study observed water diffusion coefficients in TADPS-TPA and Celazole® correlated more closely with FFV than FFV* [32]. It should be noted that, in previous work, FFV in Equation (7) was termed “water-accessible FFV,” and FFV* in Equation (8) was simply termed “FFV.” [32].

A precise value of the amount of FFV accessible for chain motion and

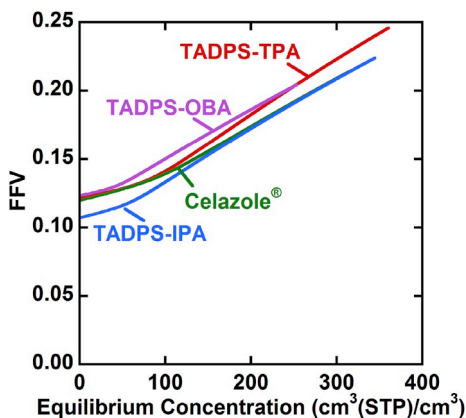


Fig. 6. Fractional free volumes (FFV) in PBIs as a function of equilibrium water concentration calculated using dual-mode sorption and dilation parameters using Equation (7). Celazole® and TADPS-TPA data are from previous study [32].

molecular diffusion in water-swollen PBIs over a time scale relevant to diffusion is difficult to characterize. Sorbed water molecules may contribute partially to reducing static free volume and partially to increasing dynamic free volume, and different water species (i.e., strongly vs. weakly bound) may affect free volume differently [23]. Future studies using microscopic techniques, such as PALS, could help elucidate the roles of static and dynamic contributions to free volume for diffusion in plasticized PBIs. For the present study, we have chosen to correlate water diffusion coefficients with FFV defined using Equation (7), since it seems more reasonable to correlate an increase in diffusion coefficients with an increase, rather than a decrease, in free volume [32]. In this case, the volume occupied by water molecules is considered to contribute to dynamic free volume and is assumed to be as equally accessible for water diffusion as unoccupied free volume. In the following section, we explore in more detail the relationship between concentration, free volume, and water diffusion in PBIs by examining how dual-mode behavior affects the concentration and free volume dependence of water diffusion.

3.5. Analysis of diffusion in PBIs

There are different ways water diffusion coefficients in polymers can be defined. In the limit of low concentration, a *local* (or mutual) diffusion coefficient can be defined using Fick's law by relating the molar flux of a penetrant to its concentration gradient [6]:

$$J_w = -D_{loc} \frac{\partial C_w}{\partial x} \quad (9)$$

where J_w is the molar flux of water (mol/cm²s), D_{loc} is the local diffusion coefficient (cm²/s), and C_w is the local water concentration (mol/cm³) at any position x in the polymer. An *average effective* diffusion coefficient, $D_{avg,eff}$, can be defined that takes into account frame of reference effects and the fact that experimental diffusion coefficients are averaged over a range of concentrations experienced by the film during a sorption step. Furthermore, the local diffusion coefficient can be expressed as the product of a thermodynamic factor, Q , and a *local mobility* coefficient, L_{loc} (see supporting information for derivations) [3,6,30,81–84].

The partial immobilization model proposed by Petropoulos [28,29] and further developed by Paul and Koros [30,31] assumes that Henry's law and Langmuir species diffuse independently with different diffusion coefficients. The local mobility coefficient is a concentration-weighted average of the local mobility coefficients of the Henry's law and Langmuir species:

$$D_{loc} = Q \cdot L_{loc} = Q \cdot \left(\frac{C_D}{C} L_{loc,D} + \frac{C_H}{C} L_{loc,H} \right) \quad (10)$$

where C_D , C_H , and C are Henry's law, Langmuir, and total concentrations, respectively (mol/cm³), and $L_{loc,D}$ and $L_{loc,H}$ are local Henry's law and Langmuir mobility coefficients, respectively (cm²/s). Previous studies have considered penetrant mobility to follow an exponential dependence with concentration, where high concentrations of sorbed penetrant significantly increase their mobility coefficients due to plasticization [22,85–89]. Since penetrant mobility is also known to be a function of the polymer's FFV, we attempt to combine both concentration and free volume dependencies into one term. Thus, we hypothesize that the local Henry's law mobility coefficient follows an exponential relationship with FFV:

$$L_{loc,D} = L_{loc,D,0} \exp\left(\frac{-B}{FFV}\right) \quad (11)$$

where $L_{loc,D,0}$ and B are empirical constants. FFV is defined according to Equation (7), where unoccupied and water-occupied volume are considered equally accessible for water diffusion. The local Langmuir mobility coefficient, $L_{loc,H}$, is assumed to be constant [29]. While this

assumption requires additional verification, Langmuir mobilities are often much smaller than Henry's law mobilities [31] and may not be affected significantly by plasticization.

As shown in the [supporting information](#), the average effective diffusion coefficient can thus be expressed as a function of water concentration and FFV:

$$D_{avg,eff} = \frac{1}{C_2 - C_1} \int_{C_1}^{C_2} \frac{Q \cdot \left[\frac{C_D}{C} L_{loc,D,0} \exp\left(\frac{-B}{FFV}\right) + \frac{C_H}{C} L_{loc,H} \right]}{1 - w_w} dC \quad (12)$$

Equation (12) can be used to describe experimental diffusion coefficients using three fitting parameters: $L_{loc,D,0}$, B , and $L_{loc,H}$. These parameters were evaluated using nonlinear least-squares regression and numerical integration and are reported in [Table 3](#). Parameter uncertainties were not estimated, since estimation was complicated by the method used for numerical integration.

[Fig. 7](#) presents experimental diffusion coefficients and corresponding model fits using Equation (12) on a log scale against $1/FFV$. Equilibrium concentrations increase moving up and to the left on the plot. Good agreement is observed between Equation (12) and experimental diffusion coefficients across the entire concentration range. If experimental diffusion coefficients were fit to Equation (5), a linear trend would be observed. However, the experimental data exhibit some deviations from linearity, which are captured by Equation (12). Thus, it is possible to describe the concentration-dependence of water diffusion coefficients by simultaneously taking into account the free volume dependency of mobility of Henry's law species, partial immobilization of Langmuir species, thermodynamic and frame of reference contributions to diffusion, and concentration averaging across the sorption interval.

The concentration dependence of each water diffusion coefficient is shown in [Fig. 8](#) for TADPS-OBA. Similar plots for other PBIs are provided in the [supporting information](#). Each diffusion coefficient was calculated using three fitting parameters for Equation (12) ($L_{loc,D,0}$, B , and $L_{loc,H}$), three dual-mode sorption parameters (k_D , C_H , and b), and two dual-mode dilation parameters (V_D and f). Local Henry's law mobility coefficients, $L_{loc,D}$, increase with concentration and follow a similar trend with concentration as FFV (cf., [Fig. 8](#)). A small increase in mobility is observed at low concentrations due to small amounts of swelling, while a steeper linear relationship between local mobility and concentration is observed at high concentrations when more swelling occurs. The intersection of $L_{loc,D}$ with the y-axis represents the infinite dilution local Henry's law mobility coefficient, $L_{loc,D,\infty}$. These values are tabulated in [Table 3](#) for each polymer. The local Langmuir mobility coefficients, $L_{loc,H}$, were all much less than the infinite dilution local Henry's law mobility coefficients (see [Table 3](#)), which is expected due to the partial

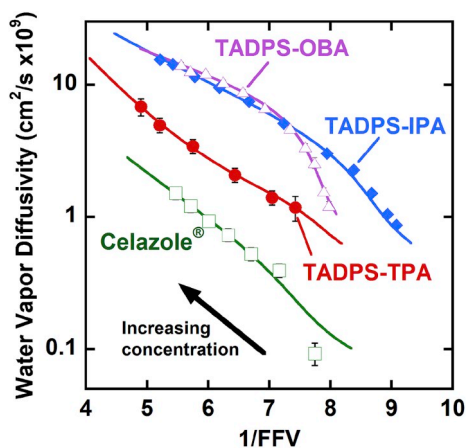


Fig. 7. Experimental water vapor diffusion coefficients vs. $1/FFV$ (defined by Equation (7)). Solid lines are curve fits using Equation (12). Equilibrium concentrations increase moving up and to the left on the plot.

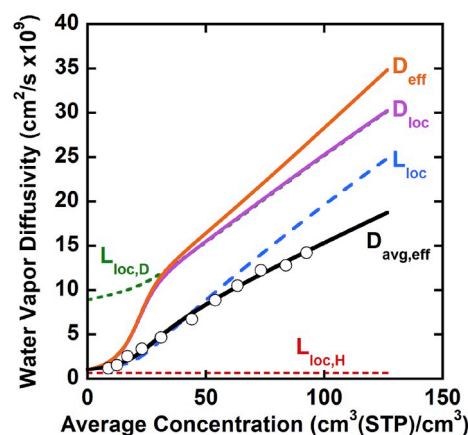


Fig. 8. TADPS-OBA water vapor diffusion and mobility coefficients vs. average water concentration in polymer. Unfilled circles represent experimental diffusion coefficients. Uncertainties are smaller than the symbols.

immobilization of Langmuir species [31]. This phenomenon has been previously observed for other polymers [31].

Values of B are expected to scale with the square of penetrant diameter [6]. Additional studies investigating penetrants other than water would be useful to establish correlations between B and penetrant size for PBIs. B also represents the sensitivity of water diffusion coefficients to free volume changes. TADPS-TPA exhibits the highest values of B , while TADPS-OBA exhibits the lowest (cf., [Table 3](#)).

Local mobility coefficients, L_{loc} , which represent a weighted average of Henry's law and Langmuir mobilities, also increase with concentration and follow a similar trend with concentration as FFV. Local diffusion coefficients, D_{loc} , follow similar trends with concentration as local mobilities with the exception of downwards curvature at average concentrations around 25–50 $\text{cm}^3(\text{STP})/\text{cm}^3$ [3]. This behavior is most evident for TADPS-OBA (cf., [Fig. 8](#)). Local diffusion coefficients are about 1–3 times greater than local mobility coefficients due to additional thermodynamic contributions to diffusion (i.e., Q). Q ranges from 1 to about 3, with values around unity at zero concentration, increasing to a maximum of 2.5–3 at average concentrations around 25–50 $\text{cm}^3(\text{STP})/\text{cm}^3$ [3], then decreasing to values around 1.2–1.5 at high concentrations (see [supporting information](#)). Similar trends have been observed for methanol in Celazole® and CO_2 in PET [80,81]. This behavior suggests strong water-polymer interactions enhance diffusion at low concentrations, as values of Q greater than unity often indicate favorable penetrant-polymer interactions [80,90]. TADPS-IPA and TADPS-OBA have only slightly higher values of Q than TADPS-TPA and Celazole®. This behavior suggests the higher diffusion coefficients of TADPS-IPA and TADPS-OBA relative to TADPS-TPA and Celazole® are due primarily to increases in mobility from enhanced chain flexibility and not primarily from enhanced sorption thermodynamics.

Effective diffusion coefficients, D_{eff} , are nearly identical to local diffusion coefficients at low concentrations and deviate upward at higher concentrations. This behavior indicates convection is essentially negligible in the low concentration limit, where it could reasonably be ignored. However, at high vapor activities where the polymers are more swollen, convection increases effective diffusion coefficients by 15–20%. Convective effects are often neglected in vapor diffusion studies, but these results indicate the importance of including convection when measuring vapor diffusion in plasticized polymers. Finally, average effective diffusion coefficients, $D_{avg,eff}$, follow similar trends to D_{eff} but are about half the value due to averaging over a concentration range of zero to equilibrium concentration. Infinite dilution average effective diffusion coefficients (D_∞) are calculated by extrapolating $D_{avg,eff}$ to zero concentration and are tabulated in [Table 3](#).

4. Conclusions

Water vapor sorption and dilation in Celazole® and three sulfone-containing PBIs follow dual-mode behavior. TADPS-OBA exhibited the lowest water uptake and degree of swelling among the four PBIs, consistent with its lower density of strong hydrogen bonding sites. Celazole® exhibited higher Langmuir capacities and lower Henry's law solubilities than its sulfone-containing analog, TADPS-IPA, likely due to a combination of more strong hydrogen bonding sites available at low concentrations and decreased chain flexibility at high concentrations.

Furthermore, a model was developed to describe the concentration-dependence of water diffusion coefficients by simultaneously taking into account the free volume dependency of mobility of Henry's law species, partial immobilization of Langmuir species, thermodynamic and frame of reference contributions to diffusion, and concentration averaging across the sorption interval. This model yielded good fits for water diffusion coefficients across a wide range of vapor activities for all four PBIs using three fitting parameters. Henry's law mobility coefficients were assumed to scale with fractional free volume (FFV), which was defined such that the volume of sorbed water was considered accessible for penetrant diffusion. This definition attempts to account for the influence of both filling pre-existing free volume elements and increasing chain mobility and dynamics on free volume and diffusion in water-swollen glassy polymers. The local mobility coefficient of water was described as a weighted average of Henry's law and Langmuir mobility coefficients. At low concentrations, local mobility coefficients were suppressed by partial immobilization of Langmuir species, while at high concentrations, mobility coefficients increased due to significant swelling and plasticization. Extension of this analysis to other plasticized polymer/penetrant systems could provide detailed insight into the individual phenomena influencing the relation between molecular diffusion and free volume in other plasticized glassy polymers.

Author contributions

The manuscript was written through contributions of all authors. All authors have given approval to the final version of the manuscript.

Funding sources

The materials, supplies, conference travel, and a portion of B.D.F.'s time was supported by the U.S. Department of Energy Office of Science, Office of Basic Energy Sciences under Award Number DE-FG02-02ER15362. B.D.F.'s role in supervising the research from January to July 2017 was partially supported by the Australian-American Fulbright Commission for the award to B.D.F. of the U.S. Fulbright Distinguished Chair in Science, Technology and Innovation sponsored by the Commonwealth Scientific and Industrial Research Organization (CSIRO). J.D.M.'s work on this research project was supported in part by the National Science Foundation Graduate Research Fellowship Program under Grant No. DGE-1610403.

Declaration of competing interest

The authors declare that they have no known competing financial interests or personal relationships that could have appeared to influence the work reported in this paper.

CRediT authorship contribution statement

Joshua D. Moon: Conceptualization, Methodology, Software, Formal analysis, Investigation, Writing - original draft, Writing - review & editing. **Michele Galizia:** Conceptualization, Methodology, Investigation, Writing - review & editing. **Hailun Borjigin:** Resources. **Ran Liu:** Resources. **Judy S. Riffle:** Resources, Writing - review & editing. **Benny D. Freeman:** Conceptualization, Methodology, Writing - review

& editing, Supervision, Project administration, Funding acquisition. **Donald R. Paul:** Conceptualization, Methodology, Writing - review & editing.

Appendix A. Supplementary data

Supplementary data to this article can be found online at <https://doi.org/10.1016/j.polymer.2020.122170>.

References

- [1] M.H. Cohen, D. Turnbull, Molecular transport in liquids and glasses, *J. Chem. Phys.* 31 (1959) 1164–1169.
- [2] J.S. Vrentas, J.L. Duda, Diffusion in polymer–solvent systems. I. Reexamination of the free-volume theory, *J. Polym. Sci. Polym. Phys. Ed* 15 (1977) 403–416.
- [3] H. Fujita, In Diffusion in Polymer-Diluent Systems, Springer Berlin Heidelberg, 1961, pp. 1–47.
- [4] J.D. Wind, S.M. Sirard, D.R. Paul, P.F. Green, K.P. Johnston, W.J. Koros, Carbon dioxide-induced plasticization of polyimide membranes: Pseudo-equilibrium relationships of diffusion, sorption, and swelling, *Macromolecules* 36 (2003) 6433–6441.
- [5] W.W. Brandt, Model calculation of the temperature dependence of small molecule diffusion in high polymers, *J. Phys. Chem.* 63 (1959) 1080–1084.
- [6] H. Lin, B.D. Freeman, Gas permeation and diffusion in cross-linked poly(ethylene glycol diacrylate), *Macromolecules* 39 (2006) 3568–3580.
- [7] A. Peterlin, Transport properties as an extremely sensitive indicator of the status of the amorphous component in the elastically and plastically deformed semicrystalline polymer, in: Interrelations between Processing Structure and Properties of Polymeric Materials, Elsevier Science Publishers B.V., Amsterdam, 1984, pp. 585–604.
- [8] R.E. Robertson, Effect of free volume fluctuations on polymer relaxation in the glassy state. II. Calculated results, *J. Polym. Sci. Polym. Phys. Ed* 17 (4) (1979) 597–613.
- [9] M.R. Tant, G.L. Wilkes, An overview of the nonequilibrium behavior of polymer glasses, *Polym. Eng. Sci.* 21 (14) (1981) 874–895.
- [10] D. Meng, K. Zhang, S.K. Kumar, Size-dependent penetrant diffusion in polymer glasses, *Soft Matter* 14 (21) (2018) 4226–4230.
- [11] K. Zhang, D. Meng, F. Müller-Plathe, S.K. Kumar, Coarse-grained molecular dynamics simulation of activated penetrant transport in glassy polymers, *Soft Matter* 14 (3) (2018) 440–447.
- [12] M. Forsyth, P. Meakin, D.R. MacFarlane, A.J. Hill, Positron annihilation lifetime spectroscopy as a probe of free volume in plasticized solid polymer electrolytes, *Electrochim. Acta* 40 (13) (1995) 2349–2351.
- [13] J.S. Vrentas, C.M. Vrentas, Solvent self-diffusion in glassy polymer-solvent systems, *Macromolecules* 27 (20) (1994) 5570–5576.
- [14] D.R. Paul, Gas sorption and transport in glassy polymers, *Ber. Bunsen Ges. Phys. Chem.* 83 (1979) 294–302.
- [15] N. Muruganandam, W.J. Koros, D.R. Paul, Gas sorption and transport in substituted polycarbonates, *J. Polym. Sci. B Polym. Phys.* 25 (1987) 1999–2026.
- [16] A. Morisato, N.R. Miranda, B.D. Freeman, H.B. Hopfenberg, G. Costa, A. Grosso, S. Russo, The influence of chain configuration and, in turn, chain packing on the sorption and transport properties of poly(tert-butyl acrylate), *J. Appl. Polym. Sci.* 49 (1993) 2065–2074.
- [17] W.J. Koros, D.R. Paul, CO₂ sorption in poly(ethylene terephthalate) above and below the glass transition, *J. Polym. Sci. Polym. Phys. Ed* 16 (11) (1978) 1947–1963.
- [18] M. Forsyth, P. Meakin, D.R. MacFarlane, A.J. Hill, Free volume and conductivity of plasticized polyether-urethane solid polymer electrolytes, *J. Phys. Condens. Matter* 7 (39) (1995) 7601–7617.
- [19] X. Hong, Y.C. Jean, H. Yang, S.S. Jordan, W.J. Koros, Free-volume hole properties of gas-exposed polycarbonate studied by positron annihilation lifetime spectroscopy, *Macromolecules* 29 (24) (1996) 7859–7864.
- [20] H. Chen, M.-L. Cheng, Y.C. Jean, L.J. Lee, J. Yang, Effect of CO₂ exposure on free volumes in polystyrene studied by positron annihilation spectroscopy, *J. Polym. Sci. B Polym. Phys.* 46 (4) (2008) 388–405.
- [21] N.R. Horn, D.R. Paul, Carbon dioxide plasticization and conditioning effects in thick vs. thin glassy polymer films, *Polymer* 52 (7) (2011) 1619–1627.
- [22] M. Minelli, M.G.D. Angelis, G.C. Sarti, Predictive calculations of gas solubility and permeability in glassy polymeric membranes: an overview, *Front. Chem. Sci. Eng.* 11 (2017) 405–413.
- [23] R.M. Hodge, T.J. Bastow, G.H. Edward, G.P. Simon, A.J. Hill, Free volume and the mechanism of plasticization in water-swollen poly(vinyl alcohol), *Macromolecules* 29 (1996) 8137–8143.
- [24] G. Dlubek, F. Redmann, R. Krause-Rehberg, Humidity-induced plasticization and antiplasticization of polyamide 6: a positron lifetime study of the local free volume, *J. Appl. Polym. Sci.* 84 (2002) 244–255.
- [25] R.J. Elwell, R.A. Pethrick, Positron annihilation studies of poly(methyl methacrylate) plasticized with dicyclohexyl phthalate, *Eur. Polym. J.* 26 (8) (1990) 853–856.
- [26] N.R. Horn, D.R. Paul, Carbon dioxide sorption and plasticization of thin glassy polymer films tracked by optical methods, *Macromolecules* 45 (6) (2012) 2820–2834.

- [27] L. Ansaloni, M. Minelli, M.G. Baschetti, G.C. Sarti, Effect of relative humidity and temperature on gas transport in Matrimid®: experimental study and modeling, *J. Membr. Sci.* 471 (2014) 392–401.
- [28] J.H. Petropoulos, Quantitative analysis of gaseous diffusion in glassy polymers, *J. Polym. Sci. A-2 Polym. Phys.* 8 (10) (1970) 1797–1801.
- [29] J.H. Petropoulos, On the dual mode gas transport model for glassy polymers, *J. Polym. Sci. B Polym. Phys.* 26 (1988) 1009–1020.
- [30] D.R. Paul, W.J. Koros, Effect of partially immobilizing sorption on permeability and the diffusion time lag, *J. Polym. Sci. Polym. Phys. Ed* 14 (1976) 675–685.
- [31] W.J. Koros, D.R. Paul, Transient and steady-state permeation in poly(ethylene terephthalate) above and below the glass transition, *J. Polym. Sci. Polym. Phys. Ed* 16 (12) (1978) 2171–2187.
- [32] J.D. Moon, M. Galizia, H. Borjigin, R. Liu, J.S. Riffle, B.D. Freeman, D.R. Paul, Water vapor sorption, diffusion, and dilation in polybenzimidazoles, *Macromolecules* 51 (18) (2018) 7197–7208.
- [33] K.A. Berchtold, R.P. Singh, J.S. Young, K.W. Dudeck, Polybenzimidazole composite membranes for high temperature synthesis gas separations, *J. Membr. Sci.* 415–416 (2012) 265–270.
- [34] X. Li, R.P. Singh, K.W. Dudeck, K.A. Berchtold, B.C. Benicewicz, Influence of polybenzimidazole main chain structure on H₂/CO₂ separation at elevated temperatures, *J. Membr. Sci.* 461 (2014) 59–68.
- [35] D.R. Pesiri, B. Jorgensen, R.C. Dye, Thermal optimization of polybenzimidazole meniscus membranes for the separation of hydrogen, methane, and carbon dioxide, *J. Membr. Sci.* 218 (2003) 11–18.
- [36] S.C. Kumbharkar, Y. Liu, K. Li, High performance polybenzimidazole based asymmetric hollow fibre membranes for H₂/CO₂ separation, *J. Membr. Sci.* 375 (2011) 231–240.
- [37] S.C. Kumbharkar, K. Li, Structurally modified polybenzimidazole hollow fibre membranes with enhanced gas permeation properties, *J. Membr. Sci.* 415–416 (2012) 793–800.
- [38] H. Borjigin, K.A. Stevens, R. Liu, J.D. Moon, A.T. Shaver, S. Swinnea, B.D. Freeman, J.S. Riffle, J.E. McGrath, Synthesis and characterization of polybenzimidazoles derived from tetraaminodiphenylsulfone for high temperature gas separation membranes, *Polymer* 71 (2015) 135–142.
- [39] S.C. Kumbharkar, P.B. Karadkar, U.K. Kharul, Enhancement of gas permeation properties of polybenzimidazoles by systematic structure architecture, *J. Membr. Sci.* 286 (2006) 161–169.
- [40] S.C. Kumbharkar, U.K. Kharul, N-substitution of polybenzimidazoles: synthesis and evaluation of physical properties, *Eur. Polym. J.* 45 (2009) 3363–3371.
- [41] N.W. Brooks, R.A. Duckett, J. Rose, I.M. Ward, An n.m.r. study of absorbed water in polybenzimidazole, *Polymer* 34 (1993) 4038–4042.
- [42] T.-S. Chung, A critical review of polybenzimidazoles, *J. Macromol. Sci., Part C* 37 (1997) 277–301.
- [43] P. Musto, P. La Manna, J.D. Moon, M. Galizia, B.D. Freeman, Infrared spectroscopy of polybenzimidazole in the dry and hydrate forms: a combined experimental and computational study, *ACS Omega* 3 (9) (2018) 11592–11607.
- [44] S.K. Burgess, D.S. Mikkilineni, D.B. Yu, D.J. Kim, C.R. Mubarak, R.M. Krieger, W. J. Koros, Water sorption in poly(ethylene furanate) compared to poly(ethylene terephthalate). Part 1: equilibrium sorption, *Polymer* 55 (2014) 6861–6869.
- [45] A. Singh, B.D. Freeman, I. Pinnau, Pure and mixed gas acetone/nitrogen permeation properties of polydimethylsiloxane (PDMS), *J. Polym. Sci. B Polym. Phys.* 36 (1998) 289–301.
- [46] S.N. Dhoot, B.D. Freeman, Kinetic gravimetric sorption of low volatility gases and vapors in polymers, *Rev. Sci. Instrum.* 74 (2003) 5173–5178.
- [47] R.D. Raharjo, B.D. Freeman, E.S. Sanders, Pure and mixed gas CH₄ and n-C₄H₁₀ sorption and dilation in poly(1-trimethylsilyl-1-propyne), *Polymer* 48 (2007) 6097–6114.
- [48] R.D. Raharjo, B.D. Freeman, E.S. Sanders, Pure and mixed gas CH₄ and n-C₄H₁₀ sorption and dilation in poly(dimethylsiloxane), *J. Membr. Sci.* 292 (2007) 45–61.
- [49] Y. Kamiya, T. Hirose, Y. Naito, K. Mizoguchi, Sorptive dilation of polysulfone and poly(ethylene terephthalate) films by high-pressure carbon dioxide, *J. Polym. Sci. B Polym. Phys.* 26 (1988) 159–177.
- [50] D. Halliday, R. Resnick, J. Walker, *Fundamentals of Physics*, John Wiley & Sons, 2010.
- [51] R.R. Tiwari, Z.P. Smith, H. Lin, B.D. Freeman, D.R. Paul, Gas permeation in thin films of “high free-volume” glassy perfluoropolymers: Part II. CO₂ plasticization and sorption, *Polymer* 61 (2015) 1–14.
- [52] S. Kanehashi, K. Nagai, Analysis of dual-mode model parameters for gas sorption in glassy polymers, *J. Membr. Sci.* 253 (2005) 117–138.
- [53] S. Matteucci, Y. Yampolskii, B.D. Freeman, I. Pinnau, Transport of gases and vapors in glassy and rubbery polymers, in: *Materials Science of Membranes for Gas and Vapor Separation*, John Wiley & Sons, Chichester, U.K., 2006, pp. 1–47.
- [54] A. Bondi, van der Waals volumes and radii, *J. Phys. Chem.* 68 (1964) 441–451.
- [55] J.Y. Park, D.R. Paul, Correlation and prediction of gas permeability in glassy polymer membrane materials via a modified free volume based group contribution method, *J. Membr. Sci.* 125 (1997) 23–39.
- [56] D.W. Tomlin, A.V. Frattini, M. Hunsaker, W. Wade Adams, The role of hydrogen bonding in rigid-rod polymers: the crystal structure of a polybenzobisimidazole model compound, *Polymer* 41 (2000) 9003–9010.
- [57] P. Musto, F.E. Karasz, W.J. MacKnight, Hydrogen bonding in polybenzimidazole/polyimide systems: a Fourier-transform infra-red investigation using low-molecular-weight monofunctional probes, *Polymer* 30 (1989) 1012–1021.
- [58] N.E. Iwamoto, Molecular Modeling Study on the Mechanical Properties of Polybenzimidazole, NAWCWPNS, 1992.
- [59] G.K. Fleming, W.J. Koros, Carbon dioxide conditioning effects on sorption and volume dilation behavior for bisphenol A-polycarbonate, *Macromolecules* 23 (1990) 1353–1360.
- [60] D. Punsalan, W.J. Koros, Drifts in penetrant partial molar volumes in glassy polymers due to physical aging, *Polymer* 46 (2005) 10214–10220.
- [61] M. Galizia, M.G. De Angelis, E. Finkelstein, Y.P. Yampolskii, G.C. Sarti, Sorption and transport of hydrocarbons and alcohols in addition-type poly(trimethyl silyl norbornene). I: experimental data, *J. Membr. Sci.* 385–386 (2011) 141–153.
- [62] D.S. Pope, W.J. Koros, H.B. Hopfenberg, Sorption and dilation of poly(1-(trimethylsilyl)-1-propyne) by carbon dioxide and methane, *Macromolecules* 27 (1994) 5839–5844.
- [63] J.R. Scherer, B.A. Bolton, Water in polymer membranes. 5. On the existence of pores and voids, *J. Phys. Chem.* 89 (1985) 3535–3540.
- [64] J. Crank, *The Mathematics of Diffusion*, second ed., Oxford University Press, London, 1975.
- [65] G.S. Park, The glassy state and slow process anomalies, in: J. Crank, G.S. Park (Eds.), *Diffusion in Polymers*, Academic, New York, NY, 1968, pp. 141–163.
- [66] F.A. Long, D. Richman, Concentration gradients for diffusion of vapors in glassy polymers and their relation to time dependent diffusion phenomena, *J. Am. Chem. Soc.* 82 (1960) 513–519.
- [67] A.R. Berens, H.B. Hopfenberg, Diffusion and relaxation in glassy polymer powders: 2. Separation of diffusion and relaxation parameters, *Polymer* 19 (1978) 489–496.
- [68] K.A. Stevens, H. Borjigin, J.D. Moon, R. Liu, R.M. Joseph, J.S. Riffle, B.D. Freeman, Influence of temperature on gas transport properties of tetraaminodiphenylsulfone (TADPS) based polybenzimidazoles, *J. Membr. Sci.* 593 (2020) 117427.
- [69] D.F. Sanders, Z.P. Smith, R. Guo, L.M. Robeson, J.E. McGrath, D.R. Paul, B. D. Freeman, Energy-efficient polymeric gas separation membranes for a sustainable future: a review, *Polymer* 54 (2013) 4729–4761.
- [70] M.R. Pixton, D.R. Paul, Relationships between structure and transport properties for polymers with aromatic backbones, in: D.R. Paul, Y.P. Yampolskii (Eds.), *Polymeric Gas Separation Membranes*, CRC Press, Boca Raton, FL, USA, 1994, pp. 83–154.
- [71] Y. Mi, S.A. Stern, S. Trohalaki, Dependence of the gas permeability of some polyimide isomers on their intrasegmental mobility, *J. Membr. Sci.* 77 (1993) 41–48.
- [72] M.R. Coleman, W.J. Koros, Isomeric polyimides based on fluorinated dianhydrides and diamines for gas separation applications, *J. Membr. Sci.* 50 (1990) 285–297.
- [73] H. Borjigin, Q. Liu, W. Zhang, K. Gaines, J.S. Riffle, D.R. Paul, B.D. Freeman, J. E. McGrath, Synthesis and characterization of thermally rearranged (TR) polybenzoxazoles: influence of isomeric structure on gas transport properties, *Polymer* 75 (2015) 199–210.
- [74] Q. Liu, H. Borjigin, D.R. Paul, J.S. Riffle, J.E. McGrath, B.D. Freeman, Gas permeation properties of thermally rearranged (TR) isomers and their aromatic polyimide precursors, *J. Membr. Sci.* 518 (2016) 88–99.
- [75] B.E. Poling, J.M. Prausnitz, J.P. O’Connell, *The Properties of Gases and Liquids*, fifth ed., McGraw-Hill, 2001.
- [76] M.C. Ferrari, M. Galizia, M.G. De Angelis, G.C. Sarti, Gas and vapor transport in mixed matrix membranes based on amorphous Teflon AF1600 and AF2400 and fumed silica, *Ind. Eng. Chem. Res.* 49 (2010) 11920–11935.
- [77] v. Krevelen, *Volumetric properties*, in: *Properties of Polymers*, third ed., Elsevier, Amsterdam, The Netherlands, 1997.
- [78] Y. Maeda, D.R. Paul, Effect of antiplasticization on gas sorption and transport. III. Free volume interpretation, *J. Polym. Sci. B Polym. Phys.* 25 (1987) 1005–1016.
- [79] J.S. Vrentas, J.L. Duda, H.C. Ling, Antiplasticization and volumetric behavior in glassy polymers, *Macromolecules* 21 (5) (1988) 1470–1475.
- [80] K.P. Bye, V. Loianno, T.N. Pham, R. Liu, J.S. Riffle, M. Galizia, Pure and mixed fluid sorption and transport in Celazole® polybenzimidazole: effect of plasticization, *J. Membr. Sci.* 580 (2019) 235–247.
- [81] K. Ganesh, R. Nagarajan, J.L. Duda, Rate of gas transport in glassy polymers: a free volume based predictive model, *Ind. Eng. Chem. Res.* 31 (1992) 746–755.
- [82] J.L. Duda, Y.C. Ni, J.S. Vrentas, An equation relating self-diffusion and mutual diffusion coefficients in polymer-solvent systems, *Macromolecules* 12 (3) (1979) 459–462.
- [83] R.J. Bearman, On the molecular basis of some current theories of diffusion, *J. Phys. Chem.* 65 (1961) 1961–1968.
- [84] M.J. Hayes, G.S. Park, The diffusion of benzene in rubber. Part 2.—high concentration of benzene, *Trans. Faraday Soc.* 52 (1956) 949–955.
- [85] F. Daghieri, G.C. Sarti, Solubility, diffusivity, and mobility of n-pentane and ethanol in poly(1-trimethylsilyl-1-propyne), *J. Polym. Sci. B Polym. Phys.* 35 (1997) 2245–2258.
- [86] M. Galizia, K.A. Stevens, D.R. Paul, B.D. Freeman, Modeling gas permeability and diffusivity in HAB-6FDA polyimide and its thermally rearranged analogs, *J. Membr. Sci.* 537 (2017) 83–92.
- [87] M. Minelli, G.C. Sarti, Permeability and diffusivity of CO₂ in glassy polymers with and without plasticization, *J. Membr. Sci.* 435 (2013) 176–185.
- [88] J. Crank, Some methods of deducing the diffusion coefficient and its concentration dependence from sorption experiments, *Trans. Faraday Soc.* 51 (1955) 1632.
- [89] S. Zhou, S.A. Stern, The effect of plasticization on the transport of gases in and through glassy polymers, *J. Polym. Sci. B Polym. Phys.* 27 (2) (1989) 205–222.
- [90] V. Loianno, S. Luo, Q. Zhang, R. Guo, M. Galizia, Gas and water vapor sorption and diffusion in a triptycene-based polybenzoxazole: effect of temperature and pressure and predicting of mixed gas sorption, *J. Membr. Sci.* 574 (2019) 100–111.